Experiments in Fluids 25 (1998) 337–346 © Springer-Verlag 1998

High speed rotor wake total temperature measurements using a hot-film anemometer

R. T. Johnston, S. Fleeter

Abstract To develop a quantitative understanding of unsteady and interacting turbomachine flow fields, it is necessary to quantify the instantaneous efficiency of high speed turbomachines. This requires the measurement of both the unsteady velocity and total temperature variation in the exit flow of a high speed rotor. In this paper, techniques to utilize a single slant-film anemometer to measure unsteady total temperature are developed and evaluated. Then a series of preliminary experiments are performed in a high speed axial fan facility to quantify the instantaneous rotor efficiency. This is accomplished by utilizing these single slant-film methods to measure the total temperature in the rotor wakes. Results show that measurements at multiple overheats and several probe orientations are required. The simplest method proves to be useful for determining parameters used in other methods. An analysis based on King's law gives good results even when measurements are outside the calibration range. Within the calibration range, a polynomial representation of the wire response to mass flux and total temperature yields good total temperature fluctuation results. A model analysis technique is also assessed.

List of symbols

A	calibration coefficient
B	calibration coefficient
C_{ni}	calibration coefficients
e	fluctuating voltage
E	wire voltage
$f(V)$	algebraic function dependent on flow velocity
k	thermal conductivity of air determined at the film temperature
Q	wire power
R_{op}	wire operating resistance
R_o	wire resistance at 0°C
S_{To}	total temperature sensitivity
S_V	velocity sensitivity
S_ρ	density sensitivity
$S_{\rho V}$	mass flux sensitivity
T_o	fluid total temperature
T_w	wire temperature
V	effective velocity
α_s	angle between hot-film and absolute flow velocity
ρ	density
τ_R	overheat ratio based on resistance ($=R_{op}/R_o$)
τ_T	overheat ratio based on temperature ($=(T_w-T_r)/T_r$)

Superscripts

-	time averaged quantity
'	fluctuating component

Received: *13 November 1997/Accepted*: *16 February 1998*

R. T. Johnston
Pratt and Whitney, M9169-21 East Hartford, CT 06108, USA

S. Fleeter
School of Mechanical Engineering, Purdue University
West Lafayette, IN 47907, USA

Correspondence to: R. T. Johnston

This research is sponsored by the GUIde Consortium on Bladed Disk Forced Response.

1 Introduction

Turbomachine flows are inherently unsteady, with blade row interactions affecting performance, flow induced vibrations, and aeroacoustics. The effects of blade row interactions on the wakes generated by the stationary and rotating airfoil rows in multistage turbomachines are of particular importance. These interacting wakes exhibit unusual temperature related characteristics. For example, the circumferential total temperature variations downstream of a stator are due to a rectification of the rotor wakes by the stators (Kerrebrock and Mikolajczak 1970). The downstream stator tends to collect the rotor wakes on its pressure surface due to the rotor wake transport relative to the main flow. Hence, the fluid in the stator wake contains greater amounts of fluid that has undergone viscous interaction with the rotor blades. There is a similar mechanism for stationary airfoil row wakes passing through a rotating blade row. The upstream stator row potential field causes the downstream rotor blade circulation to be dependent on circumferential location. This results in a circumferential variation in the time averaged temperature and pressure in the stationary frame that are a strong functions of rotor-stator spacing and relative blade counts (Shang et al. 1993). Although the total losses in a transonic compressor may be well predicted, the detailed spanwise loss variations are not (Kerrebrock 1980), and rotor efficiencies are typically found to be lower near the casing and higher in the hub regions than predicted (Kotidis and Epstein 1991).

To develop a detailed and quantitative understanding of these unsteady and interacting internal flows, it is necessary to quantify the instantaneous efficiency of high speed rotors. This requires the measurement of the time varying velocity, total pressure, and total temperature across turbomachine blade wakes. With unsteady velocities able to be measured with hot-wire anemometry, there is a clear need to develop a reliable inexpensive method to measure the unsteady total temperature across blade wakes in high speed turbomachines.

Aspirating probes have been used to measure total temperature, concentration, and pressure downstream of a turbomachine rotor (Ng 1983; Ng and Epstein 1985). Originally developed for the measurement of temperature and gas species concentration, aspirating probes incorporate a pair of wires mounted in a channel upstream of a choked orifice. Constant Mach number flow is obtained with the presence of the choked orifice. Operation of the two wires in constant temperature mode at two different overheats allows time varying flow properties such as pressure and total temperature to be determined. The main drawbacks of this technique are that the frequency response is limited by the natural frequency of the inlet (20 kHz), the yaw angle insensitive region limited to $\pm 12.5^\circ$ (Van Zante et al. 1995), the complex probe is difficult to build and repair, and spatial resolution is limited by the physical size of its inlet.

Averaged total temperatures measured with aspirating probes agree well with those calculated using the Euler turbine equation with mean flow angles. However, comparisons using time resolved data show significant differences (Ng 1983). Determination of the unsteady total temperature using Euler's turbine equation with flow velocity and direction data is based upon assumptions that are not correct for an actual wake. Namely, in applying the Euler turbine equation for temperature calculation it is assumed that the flow is steady in the rotor relative frame and there is no energy exchange between streamtubes (Ng 1983). Simple two dimensional wake models predict that the temperature increases in the rotor blade wake. This is untrue if the relative flow angle changes in the wake region. Furthermore, real wake flows are highly three dimensional with significant radial velocities.

Hot-wire anemometry is the most widely used technique for measuring fluctuating velocities. It is based on the physical principle that the heat transfer from a heated wire to the surrounding fluid is dependent on the flow properties. Calibration and use of a resistance thermal anemometer is relatively easy to implement for an incompressible flow. However, as flow speeds increase and compressibility becomes important, the calibration and use of the anemometer becomes more complex in that the anemometer output is dependent upon the density, velocity, and total temperature.

Hot-wire anemometry can also be used to measure unsteady total temperature in turbomachine flows, perhaps requiring only a single slant-wire probe. In addition to avoiding the difficulties of the aspirating probe, other advantages of using a slant-film anemometer for turbomachine unsteady wake total temperature measurements are that these sensors are inexpensive, easily repaired, common to most laboratories, high frequency response instruments (80–100 KHz), and capable of determining three components of velocity. The only drawbacks appear to be that the error in the temperature is dependent upon the angle between the flow and the sensor and that the measurements are not taken simultaneously.

The flow field of a high speed compressor is an extreme environment for the application of this single slant-wire total temperature measurement technique. This paper is directed at developing and evaluating the techniques required to utilize a single slant-film anemometer to measure the total temperature in the exit flow field of a high speed turbomachine blade row, thereby enabling the instantaneous rotor efficiency to be determined. First, four methods to utilize a single slant-film to measure total temperature are evaluated. This is accomplished by means of experiments performed in a compressible flow hot-film calibration facility which allows density, total temperature and velocity to be varied independently. Then a series of experiments are performed in a high speed axial fan facility to quantify the instantaneous rotor efficiency. This is accomplished by measuring the total temperature in the high speed rotor wake with a single slant-film anemometer. The various single slant-film total temperature data analysis methods are implemented and assessed.

2
Axial fan facility

The Purdue Research Axial Fan facility features a 30.48 cm (12 in) diameter, 2/3 hup-tip ratio design compressor rotor which is integral with the shaft. The drive system consists of a 400 horsepower AC motor driving a variable speed magnetic clutch that drives a gearbox. Eighteen inlet guide vanes introduce swirl into a 19 blade axial flow rotor. The inlet guide vanes and rotor blades were designed with NACA 65 series profiles on circular arc meanlines. Adjustable inlet guide vanes have a nominal 10% thickness with a chord varying from 35.5 mm (1.40 in) at the hub to 53.3 mm (2.10 in) at the tip to yield a solidity of one. IGV twist distribution is designed to produce a free vortex whirl into the rotor. Rotor blade sections have a 10% to 6% hub-to-tip thickness taper, with a chord of 50.8 mm (2.00 in). For these experiments, an axial IGV-to-rotor spacing to chord ratio of $Z/C_R = 0.68$ is investigated, Fig. 1. The IGV row is indexed circumferentially, thereby enabling the IGV wake measurements to be made without circumferential probe traverses upstream and downstream of the rotor.

3
Instrumentation

A TSI 1213-20 slant hot-film probe with a measurement area of 50.8 μm × 1.0 mm is used in conjunction with a TSI IFA100

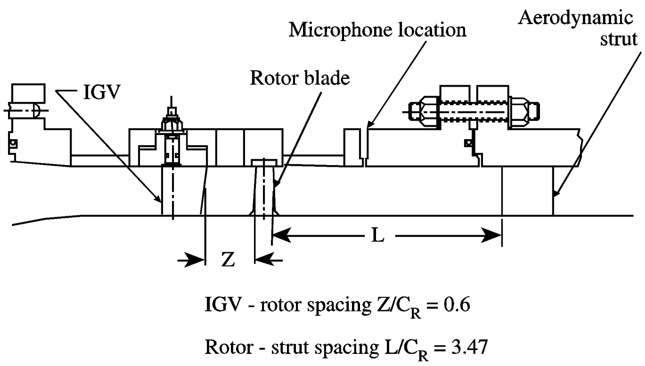

Fig. 1. Purdue high speed axial compressor research facility

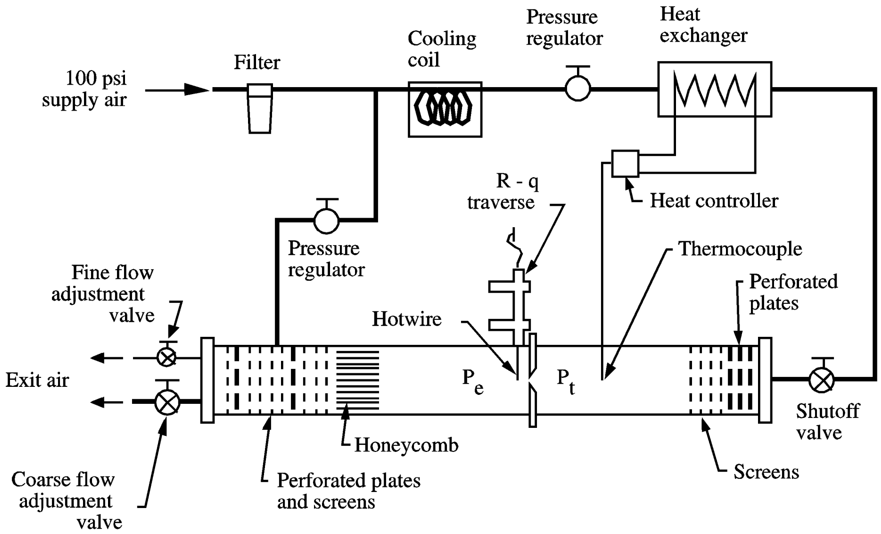

Fig. 2. Compressible flow hot-wire calibration facility

constant temperature anemometer for both the unsteady velocity and total temperature measurements. Previous high speed rotor measurements revealed that the hot-film sensor was subject to flow induced vibrations with an oscillation frequency of 25–30 kHz. This vibration was eliminated by stiffening the sensor support by adding hard epoxy around the support needles.

The difference between the wire temperatures should be as large as possible to improve independence of the how-wire data analysis equations and improve convergence. For these experiments, calibration data were taken at overheats of $\tau_r = 1.5$, 1.6, and 1.7 that correspond to wire temperatures of 194.0 °C, 232.9 °C, and 271.9 °C, respectively.

For both the velocity-direction and the total temperature measurements in the axial fan facility, measurements are triggered by a once-per-rev pulse from a photo-optic sensor and ensemble averaged over 100 individual rotor revolutions. The time varying signals are digitized over ten rotor blade passages using approximately 1000 samples per burst. An ensemble averaged signal, a RMS of the ensemble averaged signal, and an instantaneous trace are stored to disk for each wire orientation.

The three components of the velocity are determined by taking measurements at several probe orientations. For the total temperature measurements, the sensor is set to four different angles at each overheat. After determining the flow velocity and angle, the relative wire angle can be calculated for each of the temperature measurements and the one in which the relative wire angle stays nearest to 90° is selected for postprocessing.

4
Compressible hot-wire calibration facility

Problems determining hot-wire sensitivity coefficients are due to the difficulty in maintaining the density and total temperature settings and long run-times in expensive calibration facilities (Stainback et al. 1993). A calibration facility that solves this problem is shown in Fig. 2. Control of the physical properties of the calibration jet is accomplished by means of an upstream pressure chamber, an exit pressure chamber, a cooling coil, and an in-line heat exchanger with associated feed-back control. Jet total pressure is set using an instrument air pressure regulator. Exit chamber pressure is controlled by a combination of the throttling of outflow air and the addition of air. Jet flow quality is improved by the addition of perforated plates, screens, and honeycomb in both the upstream and exit pressure chambers. The jet exit diameter is 9.5 mm that affords Mach numbers up to 0.55 with the present air supply system. Standard deviations from the desired constant settings are less than 0.05% of the mean for absolute total temperature, 0.15% for velocity, and less that 0.09% for the density for the calibration data used in this report. Uncertainty of the calculated jet velocity is less than 0.1%.

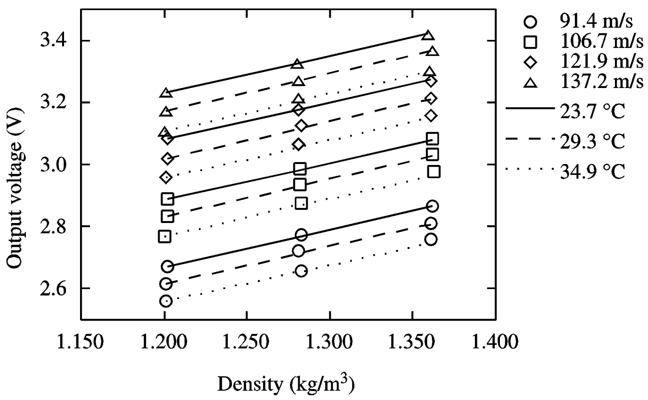

Fig. 3. Anemometer output as a function of density, total temperature, and velocity

Figure 3 shows the output from a typical sensor with the density varied from 1.2 to 1.36 kg/m^3, velocity varied from 91.4 to 137.2 m/s, and the total temperature varied from 23.7 °C to 34.9 °C. The voltage varies linearly with density for a given temperature and velocity, with a 1.2 Vm^3/kg mean slope and a standard deviation of 1.3% of the mean. These data lead to the use of a linear density correction technique for velocity measurements made with a hot-film anemometer (Johnston and Fleeter 1995). Calibration results are suitable for specification of the hot-film sensitivity coefficients S_V, S_ρ, and S_{To}

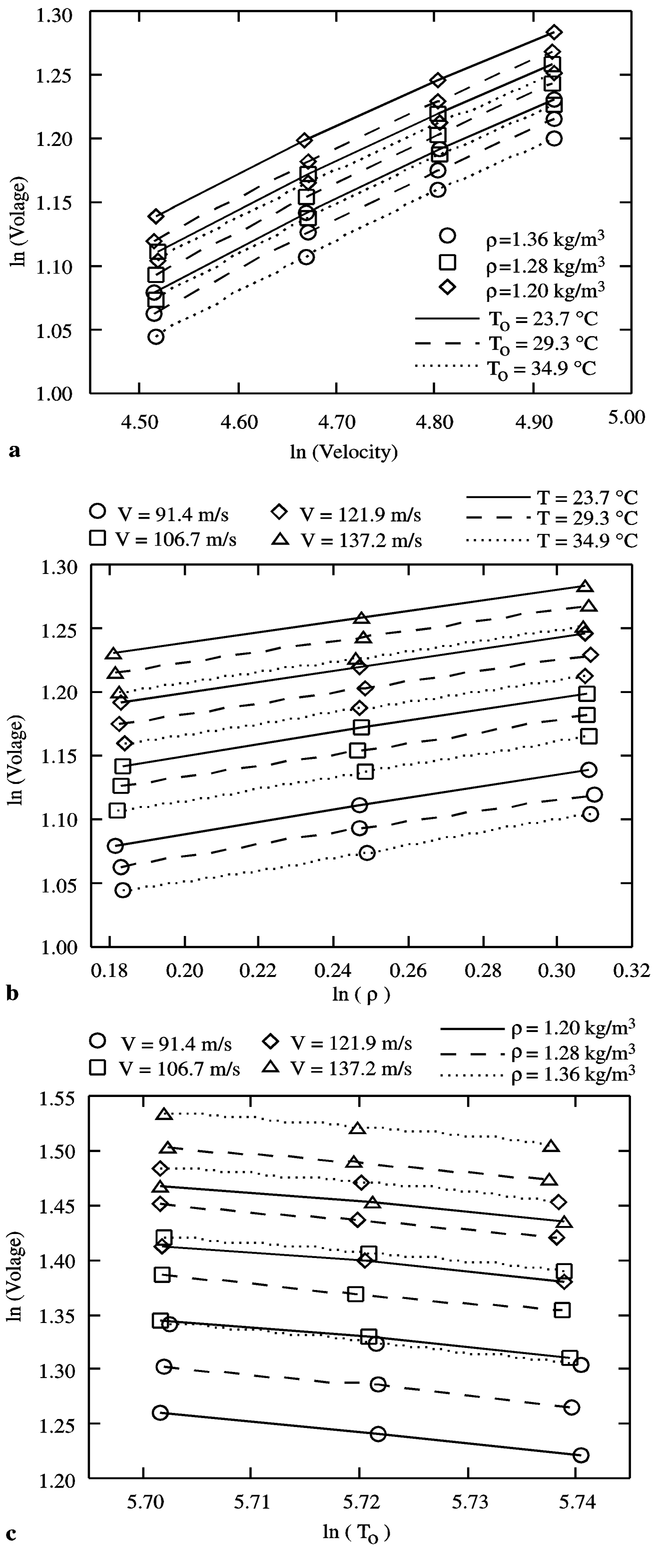

Fig. 4a–c. Calibration data for determining the sensitivity coefficients ($S_u = \partial \ln V/\partial \ln u$, $S_\rho = \partial \ln V/\partial \ln \rho$, $S_{T_o} = \partial \ln V/\partial \ln u$)

necessary to determine the axial velocity, density, and total temperature fluctuations in high speed flows. The mean slopes of the calibration data of Fig. 4 yield the sensitivity coefficients for a hot film probe with standard deviations of 2.2% for S_V, 2.2% for S_ρ, and 4.7% for S_{T_o}.

5 Total temperature data analysis

A series of experiments are performed in the compressible hot-wire calibration facility to investigate, develop, and evaluate methods to acquire and analyze slant wire data to determine the total temperature of the flow. Four data analysis methods are considered: the Power Subtraction Method, the King's Law Method, the Lienhard and Helland Method, and the Compressible Flow Modal Analysis Method.

5.1 Power subtraction method

The power subtraction method is based on a suggestion in a TSI, Inc. Bulletin (TB 16). Development of this method is included here for completeness and as a motivation for an improved method.

Wire power output is defined as

$$Q = f(V)(T_w - T_o) \tag{1}$$

where Q denotes the wire power, $f(V)$ is an algebraic function dependent on flow velocity, T_o is the fluid total temperature, and T_w the wire temperature.

Operating the wire at two overheats, the following equations are appropriate.

$$Q_1 = f_1(V)(T_{W1} - T_o) \tag{2}$$

$$Q_2 = f_2(V)(T_{W2} - T_o) \tag{3}$$

Subtracting and rearranging leads to

$$f(V) = \frac{Q_1 - Q_2}{T_{W1} - T_{W2}} \tag{4}$$

Substituting Eq. (4) into Eq. (2), the fluid total temperature is

$$T_o = T_{W1} - \frac{Q}{f(V)} \tag{5}$$

Unfortunately, the assumption that $f_1(V) = f_2(V)$ is not correct for King's Law. Thus, the power subtraction method is inherently flawed.

The data taken at the two overheats fits the following relationship.

$$E_i^2 = (C_1 + C_2(\rho V)^{0.5})(T_W - T_o) \tag{6}$$

where C_1, C_2 are calibration coefficients, E denotes the wire voltage, V the effective velocity, and ρ is the density.

For data taken at overheats of $\tau_r = 1.6$ and 1.7, the coefficients C_1 and C_2 differ by 3.8% and 15.6%, respectively. Assuming that this is acceptable, Eq. (6) then satisfies the relationship $f_1(V) = f_2(V)$ regardless of the wire temperature, and Eq. (5) becomes

$$T_o = T_{W1} - \frac{E_1^2(T_{W1} - T_{W2})}{E_1^2 - E_2^2} \tag{7}$$

Application of this relationship to the calibration data yields poor results, even with the values of T_{W1} and T_{W2} adjusted to optimize the accuracy of the calculated temperatures. Optimized wire temperatures were determined at each temperature and found to be a function of the jet total temperature (Johnston and Fleeter 1997). Results from calculations using calibration data over a density range of 1.2–1.36 kg/m³ indicate

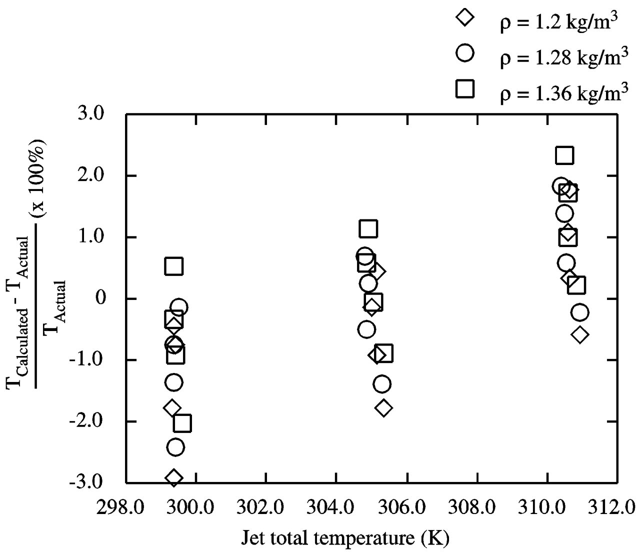

Fig. 5. Error in the calculated jet total temperature with the power subtraction method

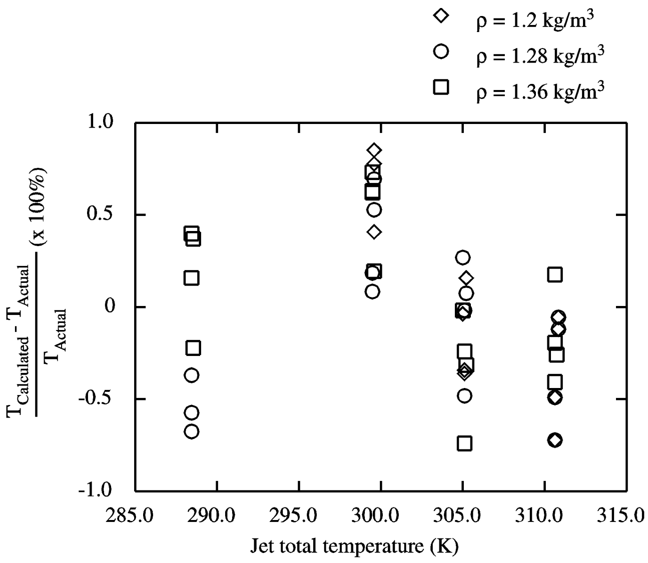

Fig. 6. Error in the calculated jet total temperature using the King's law method

that the absolute total temperature could be determined with less than 2.9% error (less than 8.7 °C). The average error was 1.0% and the RMS error was 0.7% for all data points, Fig. 5.

Since the power subtraction method is inherently flawed, it is not surprising that the calculated temperatures have errors which are relatively large. Thus, the power subtraction method provides only a rough estimate of the total temperature.

5.2
King's law method

To remove the inherent flaw in the power subtraction method, a method has been developed using King's Law. The form of King's law selected is

$$E^2 = (Ak + B(\rho V)^{0.5})(T_W - T_o) \tag{8}$$

where A, B are calibration coefficients and k denotes the thermal conductivity of air determined at the film temperature.

In order to justify the use of the ρV term in the King's law method, the heat transfer correlation from which King's law is derived must be examined:

$$\frac{hD}{k} = c + d\left(\frac{\rho VD}{\mu}\right)^{0.5} \tag{9}$$

This equation can then be rewritten as follows:

$$E^2 = [Ak + b_1 k\mu^{-0.5}(\rho V)^{0.5}]\,(T_W - T_o) \tag{10}$$

k is known to vary as $T^{0.84}$ and μ varies as $T^{0.7}$, therefore Eq. 10 can be rewritten as

$$E^2 = [Ak + b_2(\rho V)^{0.5} T^{0.49}]\,(T_W - T_o) \tag{11}$$

In order to obtain Eq. (8), the term $T^{0.49}$ is dropped from Eq. (11). The temperature dependence of B is determined from calibration to account for this variation.

With the wire operated at two overheats, two equations are obtained.

$$\frac{E_1^2 - A_1 k T_{W1}}{B_1} = T_{W1}(\rho V)^{0.5} - T_o(\rho V)^{0.5} - \frac{A_1}{B_1} k T_o \tag{12}$$

$$\frac{E_2^2 - A_2 k T_{W2}}{B_2} = T_{W2}(\rho V)^{0.5} - T_o(\rho V)^{0.5} - \frac{A_2}{B_2} k T_o \tag{13}$$

These two equations are solved simultaneously for ρV and T_o using a Newton–Raphson method.

Initial calibration results using the actual wire temperatures gave poor convergence and large errors in the calculated temperature. To reduce the differences between the calculated temperature and the actual jet temperature, the optimized wire temperatures from the power subtraction method were used. Optimized wire temperature was updated as the program converged to a solution for the jet total temperature using the curve fits of the data of for optimum wire temperature. Coefficients A and B in the King's law relationship are calculated at each total temperature. This temperature dependence of the King's Law coefficients is included in the data processing (Johnston and Fleeter 1997).

Calculated total temperature of the jet was found to have a maximum error of 0.86% (less than 2.5 °C) and a RMS error of 0.28% for data obtained in the calibration facility, Fig. 6. Calculated mass flux of the jet has a maximum error of 3.6% and a RMS error of 1.6% for the calibration data, Fig. 7. This error is considerably higher than that of the total temperature calculation and is attributed to the optimized wire temperatures being selected to provide the best accuracy in the total temperature calculation.

To address directional sensitivity, the slant-wire was transversed in 10° increments about the longitudinal axis (axis of the probe). This provides wire angles relative to the jet α_s which vary from 90°, flow normal to the wire, to 45°. Results of these calibration experiments are shown in Fig. 8 for measurements taken at two velocity and density values. Error in the calculated

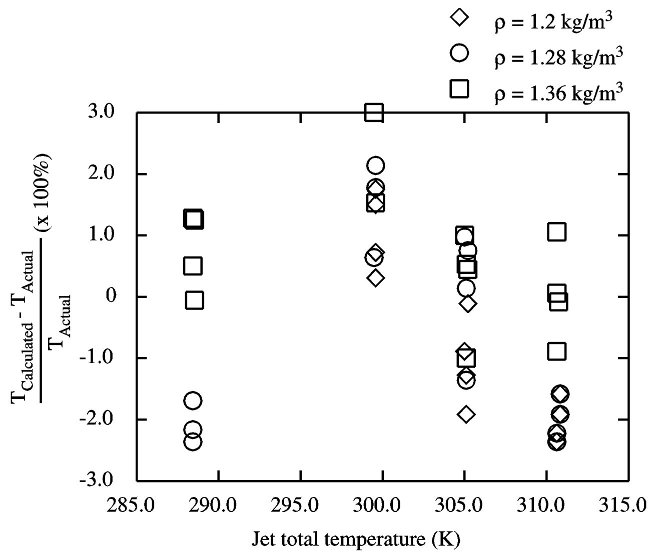

Fig. 7. Error in the calculated jet mass flux using the King's law method

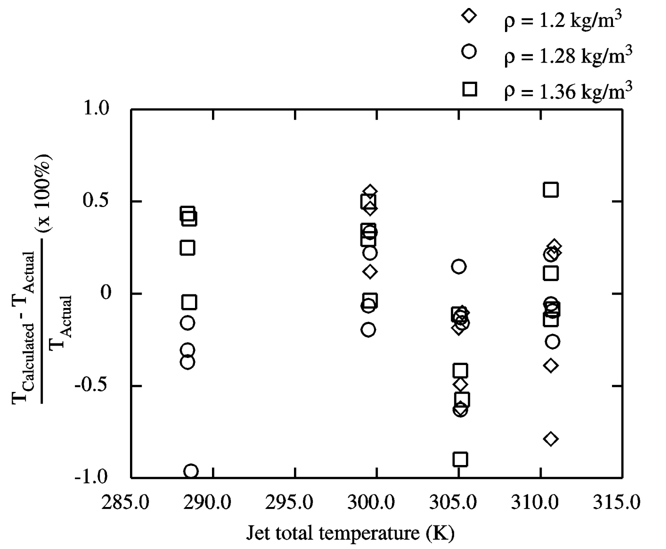

Fig. 9. Error in the calculated jet total temperature using the modified Lienhard and Helland method

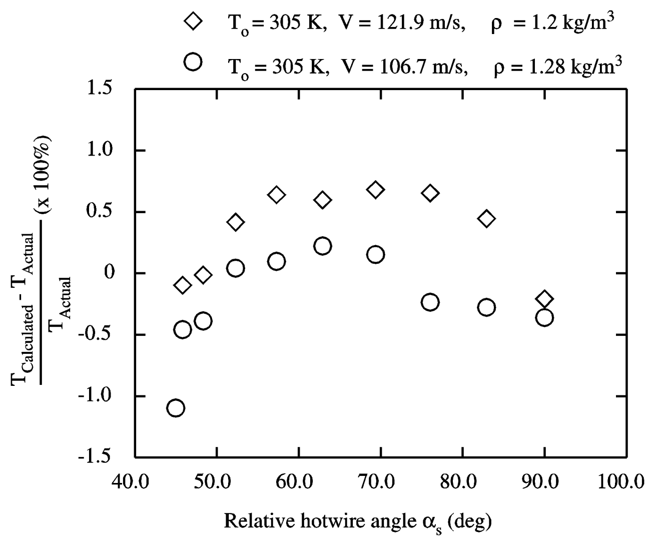

Fig. 8. Error in the calculated jet total temperature using the King's law method as a function of relative hotfilm angle α_s

temperature stays low until the relative angles α_s between the wire and the absolute velocity approach 45°. This dictates that measurements need to be taken at several wire orientations in the turbomachine and the results checked to determine whether the flow angles remain within the low error regions.

5.3
Lienhard and Helland method

The method of Lienhard and Helland (1989) to determine total temperature fluctuations defines the anemometer output voltage as a polynomial function which depends upon jet velocity and total temperature.

$$E_i^2 = C_{1i} + C_{2i}T_o + C_{3i}V^{0.45} + C_{4i}T_o^2 + C_{5i}T_oV^{0.45} \quad (14)$$

where the subscript i denotes each overheat ($i = 1, 2$).

These two equations are used to develop a single equation that can be solved for total temperature.

$$aT_o^3 + bT_o^2 + cT_o + d = 0 \quad (15)$$

Once the total temperature has been determined, the velocity can be found using Eq. (14) for one overheat.

For measurements in a compressible flow, it is necessary to account for density variations. Thus, the Lienhard and Helland method is modified by substituting the mass flux for the velocity in Eq. (14). This modification was assessed using calibration data, and good agreement with the data was obtained over the entire temperature range.

Incorrect temperatures (roots) were close to the actual temperature and the Newton–Raphson solver would converge to the wrong root if the initial guess was not closer to the actual temperature. Because of this problem with multiple roots, a two unknown Newton–Raphson solution using Eq. (14) for both overheats was implemented. Results from this modified Lienhard and Helland technique are presented in Figs. 9 and 10. Maximum relative error in the calculated absolute total temperature and mass flux are 1.0% and 2.6%, respectively.

However, this modified Lienhard and Helland method failed to converge to a solution for several test points and was found to give erroneous results for measurements taken outside the range of calibration. Thus, the modified Lienhard and Helland method is not superior to the King's law method.

5.4
Compressible flow modal analysis method

One method of interpreting the output from a hot-wire in a compressible flow is to relate the fluctuating wire voltage to the fluctuating flow properties. All quantities are divided into their fluctuating and mean values as follows:

Voltage: $E = \bar{E} + E'$

Density: $\rho = \bar{\rho} + \rho'$ (16)

Velocity: $V = \bar{V} + V'$

Total temperature: $T_o = \bar{T}_o + T_o'$

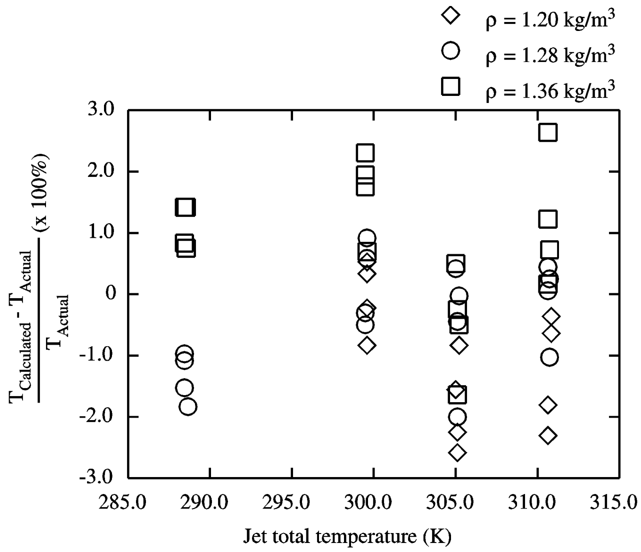

Fig. 10. Error in the calculated jet mass flux using the modified Lienhard and Helland method

These parameters are related.

$$\frac{E'}{\overline{E}} = S_\rho \frac{\rho'}{\overline{\rho}} + S_V \frac{V'}{\overline{V}} + S_{T_o} \frac{T'_o}{\overline{T}_o} \tag{17}$$

where

$$S_\rho = \left[\frac{\partial \log E}{\partial \log \rho}\right]_{V, T_o, T_w}$$

is the density sensitivity,

$$S_V = \left[\frac{\partial \log E}{\partial \log V}\right]_{\rho, T_o, T_w}$$

is the velocity sensitivity, and

$$S_{T_o} = \left[\frac{\partial \log E}{\partial \log T_o}\right]_{\rho, V, T_w}$$

is the total temperature sensitivity.

At low temperature overheat, $\tau_T < 0.4$, S_ρ, S_V, and S_{T_o} vary independently. However, when the overheat is higher, i.e., $\tau_T > 0.5$, and the wire Reynolds number is greater than 20, then S_ρ and S_V are approximately equal and constant (Horstman and Rose 1975, 1977). This leads to the following simplification of Eq. (17):

$$\frac{E'}{\overline{E}} = S_{\rho V} \frac{(\rho V)'}{\overline{\rho V}} + S_{T_o} \frac{T'_o}{\overline{T}_o} \tag{18}$$

where

$$S_{\rho V} = \left[\frac{\partial \log E}{\partial \log \rho V}\right]_{T_o, T_w}$$

is the mass flux sensitivity.

The data reduction techniques necessary to determine the fluctuating velocity, density, and total temperature when it is assumed that $S_\rho = S_V$ and when S_ρ, S_V, and S_{T_o} have all been evaluated by Stainback (1986) and are shown to yield different results. Also presented is a comparison of the errors resulting from the data analysis techniques.

If $S_\rho = S_V$, the voltage fluctuations are only related to the total temperature and mass flux fluctuations. Hence, measurements must be taken at two overheats to determine the fluctuating velocity, total temperature, and density, with the following matrix equation then solved.

$$\begin{vmatrix} \frac{m'}{m} \\ \frac{T'_o}{T_o} \end{vmatrix} = \begin{vmatrix} S_{\rho V_1} & S_{T_{o1}} \\ S_{\rho V_2} & S_{T_{o2}} \end{vmatrix}^{-1} = \begin{vmatrix} \frac{E'_1}{E_1} \\ \frac{E'_2}{E_2} \end{vmatrix} \tag{19}$$

where the subscript 1 and 2 refer to the two different overheats.

Knowing the instantaneous mass flux and total temperature, the fluctuating density and velocity can be found if it is assumed that the fluctuating pressure normalized by the mean pressure is small (Kovasznay 1950).

$$\frac{V}{\overline{V}'} = \left[\frac{1 + \frac{\gamma - 1}{2} M^2}{1 + (\gamma - 1) M^2}\right] \frac{T'_o}{T_o} + \left[\frac{1}{1 + (\gamma - 1) M^2}\right] \frac{m}{\overline{m}} \tag{20}$$

$$\frac{\rho'}{\overline{\rho}} = \left[\frac{(\gamma - 1) M^2}{1 + (\gamma - 1) M^2}\right] \frac{m'}{\overline{m}} + \left[\frac{1 + \frac{\gamma - 1}{2} M^2}{1 + (\gamma - 1) M^2}\right] \frac{T'_o}{\overline{T}_o} \tag{21}$$

A method of determining the fluctuating values of density, velocity, and total temperature when the coefficients S_ρ, S_V, and S_{T_o} at three overheats are known is given by Stainback et al. (1983). The defining equation is

$$\frac{E'_i}{\overline{E}_i} = S_{\rho i} \frac{\rho'}{\overline{\rho}} + S_{V i} \frac{V'}{\overline{V}} + S_{T_{oi}} \frac{T'_o}{\overline{T}_o}, \quad i = 1, 2, 3 \tag{22}$$

These equations can be solved for the instantaneous velocity, density, and total temperature by inverting the sensitivity coefficient matrix.

$$\begin{vmatrix} \frac{\rho'}{\overline{\rho}} \\ \frac{V'}{\overline{V}} \\ \frac{T'_o}{\overline{T}_o} \end{vmatrix} = \begin{vmatrix} S_{\rho_1} & S_{V_1} & S_{T_{o1}} \\ S_{\rho_2} & S_{V_2} & S_{T_{o2}} \\ S_{\rho_3} & S_{V_3} & S_{T_{o3}} \end{vmatrix}^{-1} \begin{vmatrix} \frac{E'_1}{\overline{E}_1} \\ \frac{E'_2}{\overline{E}_2} \\ \frac{E'_3}{\overline{E}_3} \end{vmatrix} \tag{23}$$

Note that no assumptions have been made about the pressure fluctuations. Stainback compares the results from these two methods ($S_\rho = S_V$ and $S_\rho \neq S_V$) and indicates that errors may be large if it is incorrectly assumed that $S_\rho = S_V$.

In the high speed rotor wake experiments, even though this method is not intended for flows with large fluctuations, results from Eq. (23) will be compared with results from the other methods. One main drawback of this technique is that measurements must be taken at three overheats in the rotor wake. This leads to longer calibration and run times that increases "soiling" of the hot-film and increases the chance of breakage.

6
Results

A series of experiments are performed in the high speed axial compressor facility, with the total temperature in the wake of the high speed rotor measured with a single slant-film anemometer. A high speed compressor is an extreme environment for the application of this single slant-wire total temperature measurement technique due to the high frequency fluctuations of density, velocity, and temperature. The four data analysis methods are implemented and assessed with regard to their potential for this application.

6.1
High speed rotor experiments

High speed rotor wake data are acquired and analyzed at 10000 RPM. Mass flow rate and total pressure ratio are 3.3 kg/s and 1.07 at 10000 RPM. To increase the stage temperature ratio, the exit flow is throttled, thereby decreasing the axial velocity deficit and increasing the radial velocity fluctuations. Note that at both operating conditions the radial component of velocity has a small bias, i.e., a non-zero mean.

The relative angle between the flow velocity vector and the sensor, α_s, for several probe angles is shown in Fig. 11, with the probe angle θ_y indicated. To determine the rotor wake total temperature, the data set that has near orthogonal values of α_s is selected, determined by calculating the magnitude of α_s. Considering these results, the rotor wake total temperature is determined from the $\theta_y = 80^\circ$ data.

6.2
Time varying rotor efficiency

The high speed rotor wake total temperature measured with a single slant-film method and analyzed with the power subtraction method, the King's law method, the modified Lienhard and Helland method, and the Compressible Flow Modal Analysis Method, is presented in Fig. 12.

At 10000 RPM the Kings' law, modified Lienhard and Helland, and the Modal Analysis methods are in good

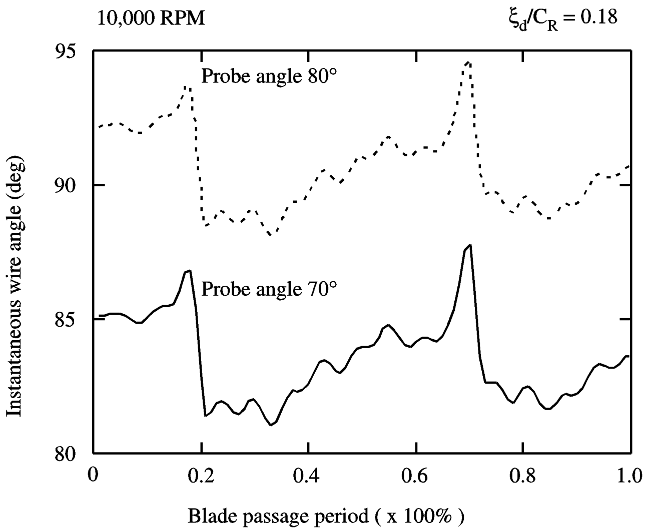

Fig. 11. Instantaneous angle between absolute velocity vector and hotfilm, α

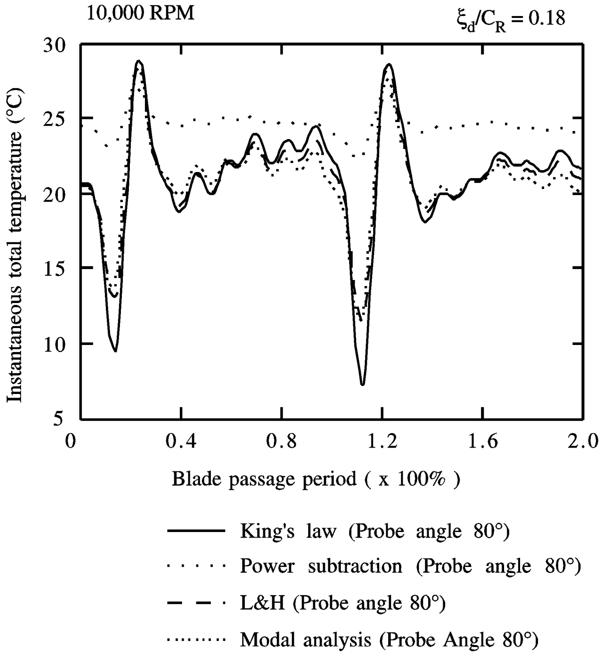

Fig. 12. Calculated total temperature in the rotor wake with different methods, 10000 RPM

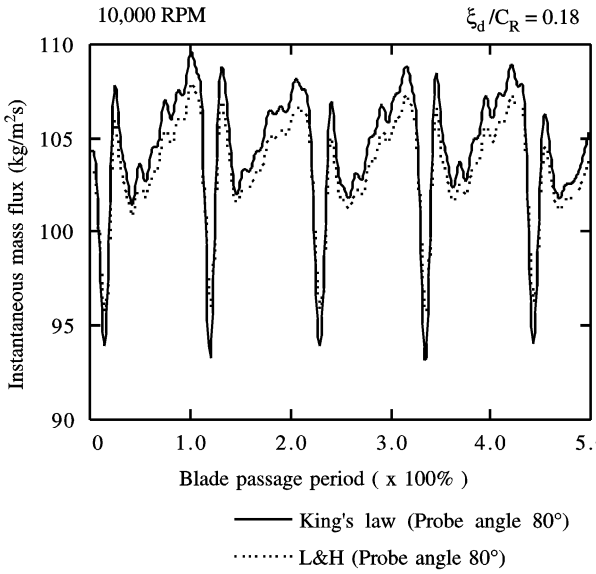

Fig. 13. Calculated mass flux in the rotor wake with different methods

agreement. The Power Subtraction method gives much lower fluctuations in total temperature than the other methods and the mean temperature has a large error at 10000 RPM. The temperature obtained by averaging five blade passes yields total temperature which is 0.4% different from the mass averaged total temperature at 10000 RPM based upon absolute temperature when using the King's law method. This good agreement between the mass averaged total temperature measured using thermocouples and the time average of the unsteady temperature is indicative of validity of the technique.

The rotor wake mass flux (ρV) calculated using the modified Lienhard and Helland technique is compared to the King's law method in Fig. 13. There is very excellent agreement between the two techniques with only a small difference in the mean values.

Notice that all of the direct measurement techniques show a decrease in temperature followed by a sharp increase in temperature across the rotor blade wake. This decrease in temperature would not be predicted if the temperature is calculated using the tangential velocity variations. This feature is also evident in measurements made by Ng (1983) and Van Zante et al. (1995). The minimum of the temperature curves corresponds to the inlet total temperature at 15 °C and occurs on the pressure surface side of the wake.

6.3
Rotor wake efficiency

To develop a detailed and quantitative understanding of these unsteady and interacting internal flows, it is necessary to quantify the instantaneous efficiency of high speed rotors. The definition used for the calculation of unsteady total-to-total efficiency presented is given in Eq. (24).

$$\eta_{tt} = \left[\frac{p_2/p_1(\gamma - 1)/\gamma - 1}{T_2/T_1 - 1} \right] \quad (24)$$

This requires the measurement of both the time varying total pressure and temperature across turbomachine blade wakes. A plot of total-to-total efficiency is shown in Fig. 14. Note that the efficiencies calculated in the unsteady flow between the IGV wakes are larger than those found in the IGV wake regions. The nature of these curves is not unlike that shown by Ng (1983) but the variation in magnitude is much larger. This large variation in efficiency is attributed to the total temperature ratio being very close to unity in this particular facility. This makes the calculated efficiency very sensitive to small temperature fluctuations and measurement errors. The regions of efficiency which are larger than one occur on the pressure side of the wake and this is in agreement with others (Ng and Epstein 1985; Van Zante et al. 1995). These efficiencies which are greater than unity have been found to exist from the hub to midspan region through both unsteady and steady measurements. With unsteady velocities able to be measured with hot-wire anemometry, there is a clear need to develop the capability to measure the unsteady total temperature across blade wakes in high speed turbomachines.

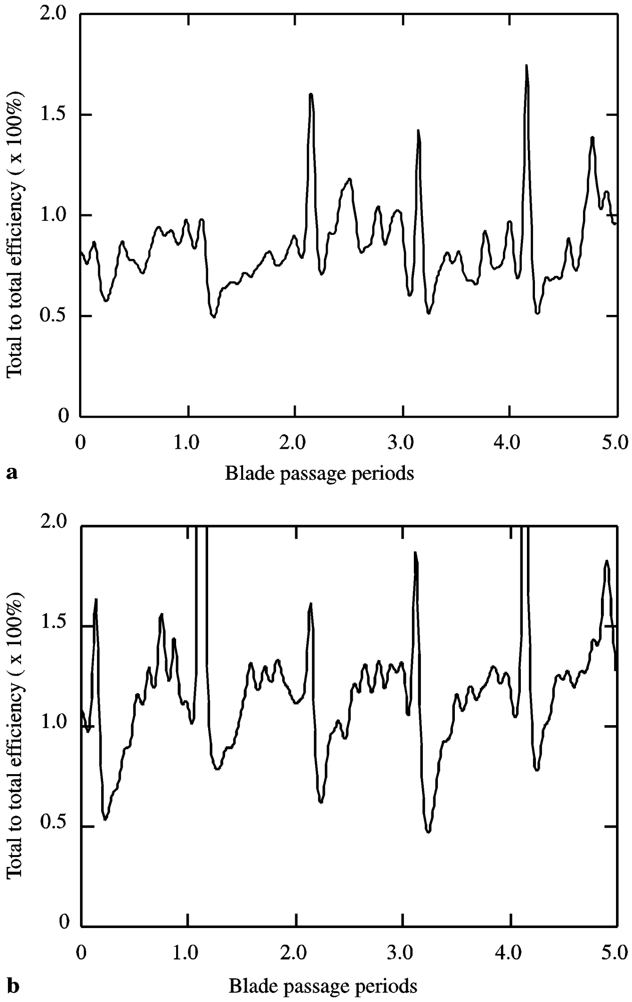

Fig. 14a, b. Instantaneous rotor efficiency. **a** in IGV wake; **b** in freestream

7
Summary and conclusions

A series of experiments were performed in a high speed axial fan facility to quantify the instantaneous efficiency of the rotor. This was accomplished by measuring the total temperature in the wake of the high speed rotor with a single slant-film anemometer, thereby enabling the instantaneous rotor efficiency to be determined. First, a compressible flow hot-film calibration facility which allows density, total temperature and velocity to be varied independently was utilized to evaluate four data analysis methods: the power subtraction method, the King's law method, the modified Lienhard and Helland method, and the compressible flow modal analysis method. The various single slant-film total temperature data analysis methods were implemented in an axial compressor and assessed. Then a series of experiments were performed in a high speed axial fan facility to quantify the instantaneous rotor efficiency.

The King's law and the Lienhard and Helland methods yielded the best results when applied to calibration data and the high speed rotor wake measurements. However, the four data analysis methods have different strengths and weaknesses.

The power subtraction method was shown to be inherently flawed and to have a large relative error in the calculated temperatures. However it does provide the value of optimized wire temperature used in the King's law analysis.

Advantages of the King's law analysis are that it accounts for density fluctuations, accurately determines temperature outside the calibration range, and is relatively insensitive to wire angle. Two drawbacks are that it requires the determination of optimized wire temperatures and that the values of the wire temperature *Tw* and the calibration constants *A* and *B* need to be updated as the solution converges.

When using the modified Lienhard and Helland Method, the density fluctuations are accounted for and it exhibits the same insensitivity to wire orientation as the King's law method. However, it cannot be used on data that are outside the calibration range due to the nature of the polynomial curve fits.

The modal analysis technique provides only the magnitude of the fluctuation and is not intended for large amplitude fluctuations. The matrix multiplication used in the total temperature solution is easy to implement, but calibrating and taking measurements at three overheats requires excessive time.

With regard to the high speed rotor wake experiments, at 10000 rpm, there is good agreement between the King's Law, modified Lienhard and Helland, and Modal Analysis methods. The Power Subtraction method does not agree with the other methods.

In summary, total temperature measurement in a high speed compressor is an extreme environment for the application of this measurement technique. The periodic nature of the flow field enables the total temperature to be determined by ensemble averaged measurements taken by a single slant-wire probe at different overheats. The advantages of using a single slant-film anemometer for these measurements are that these sensors are: inexpensive, easily repaired, common to most laboratories, high frequency response instruments (80–100 kHz), and also capable of determining three components of velocity. The only drawbacks appear to be that the error in the temperature is dependent upon the angle between the flow and the sensor and that the measurements are not simultaneous. Utilization of a multiple wire probe and experimentation with different overheat ratio combinations would be two possible improvements to this method.

References

Horstman CC; Rose WC (1977) Hot-wire anemometry in transonic flow. AIAA J 15: 395–401

Horstmann CC; Rose WC (1975) Hot-wire anemometry in transonic flow. NASA TM X-62,495

Johnston RT; Fleeter S (1995) High speed rotor wake, vortical and potential forcing functions. AIAA Paper 95-2482

Johnston RT; Fleeter S (1997) Rotor wake total temperature measurements using a hot-film anemometer. AIAA Paper 97-0601

Kerrebrock JL; Mikolajczak AA (1970) Intra-stator transport of rotor wakes and its effect on compressor performance. J Eng Power 359–368

Kerrebrock JL (1980) Flow in transonic compressors. AIAA J 19: 1–19

Kotidis PA; Epstein AH (1991) Unsteady radial transport in a transonic compressor stage. J Turbomachinery 113: 207–218

Kovasznay LS (1950) The hot-wire anemometer in supersonic flow. Journal of Aeronautical Sciences. 565–573

Lienhard JH; Helland KN (1989) An experimental analysis of fluctuation temperature measurements using hot-wires at different overheats. Exp Fluids 7: 265–270

Ng W (1983) Time resolved stagnation temperature measurement in a transonic compressor stage. MIT GTL Report 177

Ng WF; Epstein AH (1985) Unsteady losses in transonic compressors. J Eng Gas Turbines and Power 107: 345–353

Shang T; Epstein AH; Giles MG; Sehra AK (1993) Blade row interaction effects on compressor measurements. J Propulsion Power 9: 569–578

Stainback PC; Nagabushana KA; Jones GS (1993) A status report for hot-wire anemometry development at the Langley Research Center for Transonic and Subsonic Slip Flow Regimes. Thermal Anemometry, ASME FED-Vol. 167: 209–217

Stainback PC (1986) Some influences of approximate values for velocity, density, and total temperature sensitivities on hot-wire anemometer results. AIAA Paper 86-0506

Stainback PC; Johnson CB; Basnett CB (1983) Preliminary measurements of velocity, density, and total temperature fluctuations in compressible flow. AIAA Paper 83-1684

TSK Inc., temperature compensation of thermal sensors. Technical Bulletin, TB 16

Van Zante DE; Suder KL; Strazisar AJ; Okiishi TH (1995) An improved aspirating probe for total-temperature and total-pressure measurements in compressor flows. J Turbomachinery 117: 642–649